A New Statistical Wideband Spatio-Temporal Channel Model for 5-GHz Band WLAN Systems

Chia-Chin Chong, *Student Member, IEEE,* Chor-Min Tan, *Student Member, IEEE,* David I. Laurenson, *Member, IEEE,* Stephen McLaughlin, *Member, IEEE,* Mark A. Beach, *Associate Member, IEEE,* and Andrew R. Nix, *Associate Member, IEEE*

***Abstract*—In this paper, a new statistical wideband indoor channel model which incorporates both the clustering of multipath components (MPCs) and the correlation between the spatial and temporal domains is proposed. The model is derived based on measurement data collected at a carrier frequency of 5.2 GHz in three different indoor scenarios and is suitable for performance analysis of HIPERLAN/2 and IEEE802.11a systems that employ smart antenna architectures. MPC parameters are estimated using the super-resolution frequency domain Space-Alternating Generalized Expectation maximization (FD-SAGE) algorithm and clusters are identified in the spatio-temporal domain by a nonparametric density estimation procedure. The description of the clustering observed within the channel relies on two classes of parameters, namely, *intercluster* and *intracluster parameters* which characterize the cluster and MPC, respectively. All parameters are described by a set of empirical probability density functions (pdfs) derived from the measured data. The correlation properties are incorporated in two joint pdfs for cluster and MPC positions, respectively. The clustering effect also gives rise to two classes of channel power density spectra (PDS)—*intercluster* and *intracluster PDS* which are shown to exhibit exponential and Laplacian functions in the delay and angular domains, respectively. Finally, the model validity is confirmed by comparison with two existing models reported in the literature.**

***Index Terms*—Antenna array, clustering multipath channel, indoor radio communication, radio propagation, spatio-temporal correlation.**

I. Introduction

RECENTLY, wireless local-area networks (WLANs) have attracted considerable interest and attention due to their ability to provide broadband wireless communication. Several new standards have been developed in the 5-GHz band, namely the High Performance Local-Area Networks type 2 (HIPERLAN/2) defined by European Telecommunications Standards Institute (ETSI) Broadband Radio Access Networks (BRAN), 802.11a defined by IEEE and High Speed Wireless Access Network type a (HiSWANa) defined by Mobile Access Communication Systems (MMAC) [1]. These standards are capable of providing data rates of up to 54 Mb/s for short range communication in the indoor environments.

High-data rates imply the use of a large bandwidth. However, the limited radio spectrum forms the major bottleneck in achieving such high-data rates. Smart antennas (SAs) have emerged as one of the most promising candidates to maximize the wireless capacity through multiple-input-multiple-output (MIMO) antenna arrays [2]. SAs exploit both the spatial and temporal domains by means of different space–time signal processing techniques, such as the new Turbo space–time codes and various spatial-diversity schemes. Successful deployment of the SAs will require a detailed knowledge of the radio propagation channel, thus, a realistic spatio-temporal channel model is essential for the performance evaluation of any space–time processing technique and any indoor system design.

Despite many spatial channel models having been reported in the literature [3], [4], few of them incorporated both the spatial and temporal correlation properties when the models were being developed. Modeling the correlation between these two domains is essential as a strong correlation could enhance the performance of the space–time processing techniques. To the best of the authors' knowledge, only two models have appeared in the literature which provide a statistical description for the spatio-temporal properties in indoor propagation environments based on real measurement data. The first model is the extension of the Saleh–Valenzuela temporal domain only model [5] with the angle-of-arrival (AOA) information (ESVM) [6]. This model adopts the clustered double Poisson time-of-arrival (TOA) model detailed in [5] and proposes that the clustering phenomenon is also observable in the angular domain. The model was derived from the results of measured data at a carrier frequency of 7 GHz. The clusters' mean AOAs are taken to be uniformly distributed over the range [0,360]°, while the multipath components (MPCs) AOAs within each cluster are taken to be Laplacian distributed. A key assumption made in this model is that the spatial and temporal domains are independent of one another. The second model is known as the *stochastic radio channel model* (SRCM) [7]. This model was developed based on measurement data collected at a carrier frequency of 24 GHz in an office environment under both line-of-sight (LOS) and non-LOS (NLOS) scenarios. A *nonclustered* and a *clustered* model were proposed for LOS and NLOS conditions, respectively. However, none of these models investigate the spatio-temporal correlation properties of the indoor propagation channel despite its importance. Furthermore, these models were not developed specifically

Manuscript received April 26, 2002; revised September 21, 2002. This work was supported in part by Virtual Centre of Excellence in Mobile and Personal Communications (Mobile VCE).

C.-C. Chong, D. I. Laurenson, and S. McLaughlin are with the Institute for Digital Communications, University of Edinburgh, Edinburgh EH9 3JL, U.K. (e-mail: Chia-Chin.Chong@ieee.org).

C.-M. Tan, M. A. Beach, and A. R. Nix are with the Centre for Communications Research, University of Bristol, Bristol BS8 1UB, U.K. (e-mail: Chor.Min.Tan@bristol.ac.uk).

Digital Object Identifier 10.1109/JSAC.2002.807347

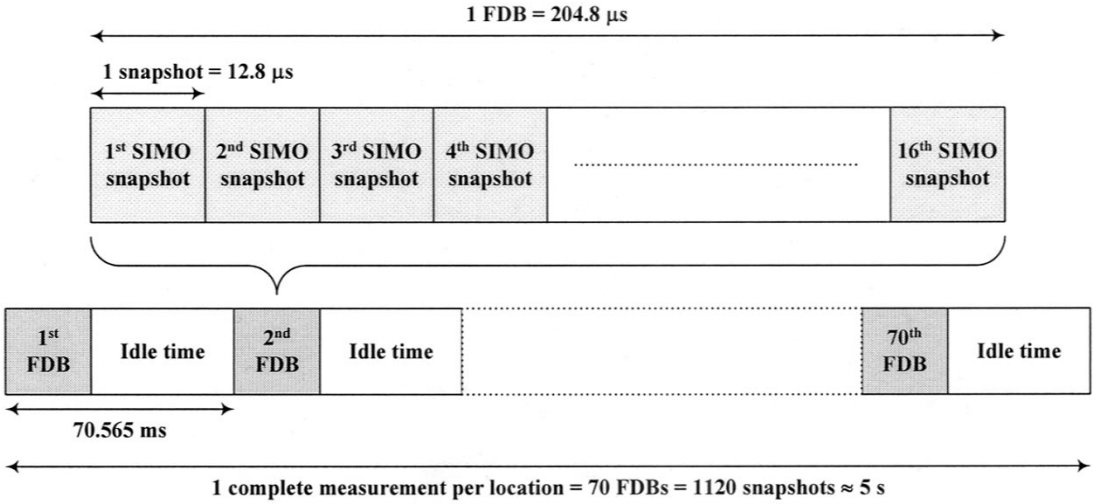

Fig. 1. Illustration of the measurement setup.

for HIPERLAN/2 or IEEE802.11a systems. To date, the most commonly deployed HIPERLAN/2 channel model is reported in [8]. Nevertheless, this model does not incorporate the spatial information necessary for the development of SA technologies.

The objectives of this paper are twofold. First, to study in more detail the statistical characteristics of the 5-GHz band WLAN channel in both spatial and temporal domains, particularly the clustering of MPCs and the correlation between these two domains. Clustering of MPCs can have a significant impact on channel capacity. Unclustered models tend to overestimate the capacity if the MPCs are indeed clustered [9]. This implies that a more comprehensive characterization of the clustering and correlation properties is required. Second, to propose a new statistical wideband spatio-temporal channel model suitable for HIPERLAN/2 and IEEE802.11a systems. The new proposed model will incorporate both the *clustering* and *correlation* properties described above and can be employed for LOS, obstructed-LOS (OLOS) and NLOS scenarios. The clustering effect gives rise to two classes of channel parameters (*intercluster* and *intracluster parameters*) and power density spectra (PDS) (*intercluster* and *intracluster PDS*) while the correlation properties are incorporated in two joint probability density functions (pdfs) for cluster and MPC positions, respectively.

The organization of the paper is as follows. Section II describes the measurement setup and environments. Section III presents the data analysis and processing techniques to extract MPC parameters and to identify clusters. In Section IV, a new spatio-temporal channel model is proposed. Sections V and VI describe in detail the statistical characteristics and PDS of the channel model. In Section VII, a comparison is made between the proposed model and existing models reported in the literature. Finally, in Section VIII, appropriate conclusions are drawn.

II. Measurement Setup and Environments

A. Measurement Setup

This section describes the indoor channel measurement campaign conducted at the University of Bristol (UoB). The wideband measurement was performed in the 5.2 GHz band using the Medav RUSK BRI vector channel sounder [10]. The periodic multifrequency test signal used in the measurement had a repetition period of 0.8 μs and a bandwidth of 120 MHz. The measurements were based on a single-input–multiple-output (SIMO) configuration with an omni-directional transmitter (TX) and an eight-element uniform linear array (ULA) receiver (RX). The ULA had eight dipole-like active elements spaced by half the wavelength and two inactive elements at each end. Its effective azimuth visible range is 120°. Both the TX and the RX were fixed at the same height in all measurements.

The sounder was set up to record 16 consecutive SIMO snapshots as a fast Doppler block (FDB), where a SIMO snapshot consists of eight complex channel responses across the ULA [10]. The channel responses were computed online and were stored on the sounder's hard disk as the complex frequency response for subsequent offline post-processing. The time required to record a SIMO snapshot and a FDB was 12.8 μs and 204.8 μs (16×12.8 μs), respectively. This guaranteed the channel responses in one FDB were recorded within the coherence time of the channel and within the 2-ms medium access control (MAC) frame of the HIPERLAN/2 system. In order to collect more samples for statistical analysis, 70 FDBs were recorded in a duration of approximately 5 s in a time grid of 70.565 ms. Therefore, one complete measurement set in each fixed-terminal location consists of a total of 1120 (16×70 SIMO snapshots. Fig. 1 illustrates the measurement setup.

B. Measurement Environments

Three different indoor environments in the UoB were chosen for the measurement campaign: Room 2.19 (OFF) and the entrance foyer (FOY) in the Merchant Venturers Building (MVB) which represent a large office and a large open space environment, respectively. In addition, the electrical laboratory (LAB) in the Queens Building (QB) was also used. The layout of OFF and FOY is shown in Fig. 2. These environments are typical indoor environments for the future WLAN deployment. For example, both OFF and LAB have a lot of computers with some fixed-wired network facilities. The initial phase of the deployment of future wireless network system will most likely take

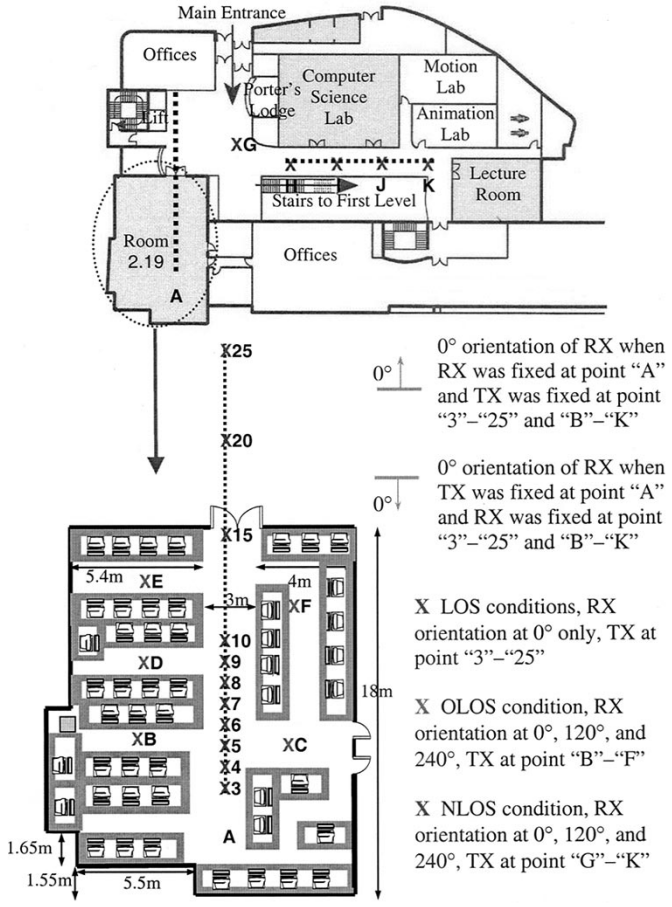

Fig. 2. Sketched plans of the (a) entrance foyer (FOY) and (b) Room 2.19 (OFF) in MVB.

place in such environments. Measurements were conducted during normal office hours with no restrictions imposed on the channel as people were free to move. Hence, the data collected and used in the analysis was obtained from a realistic indoor radio environment and the statistical model produced in this work is realistic for the simulation of future WLAN systems.

The measurements were conducted in such a way that both the TX and RX were fixed at one location when the sounder was recording the 1120 SIMO channel snapshots. These locations were carefully chosen to represent the LOS, OLOS and NLOS scenarios. During the measurement, either the TX or the RX was fixed at location "A" (refer to Fig. 2) while the other end was fixed at other locations (labeled as positions "3"–"25" and "B"–"K" in the plan). For the measurements in OFF, the LOS condition was obtained at locations "3"–"25" and the OLOS condition was obtained at locations "B"–"F," where the direct path was obstructed by wooden bookshelves, metal cabinets, and/or scatterers in the environment. All measurements in FOY were under the NLOS condition as the direct path between location "A" and locations "G"–"K" was blocked by the walls of Room 2.19. Meanwhile, all measurements in LAB were based on the LOS condition in which the TX-RX separation varied from 3 m to 45 m. The RX orientation was at 0° for the LOS scenario while three different RX orientations (0°, 120°, and 240°) were used under OLOS and NLOS scenarios in order to obtain the 360° spatial view.

III. Data Analysis and Processing

A. Channel Parameter Estimation

Before any statistical channel modeling work can be performed, the first step is to extract the channel parameters of interest from the measurement data. Two super-resolution algorithms, namely, the space-alternating generalized expectation maximization (SAGE) [11] and the unitary estimation of signal parameters via rotational invariance techniques (ESPRIT) [12], examples of maximum-likelihood (ML) and subspace- based methods, respectively, were investigated. Here, the frequency domain SAGE (FD-SAGE) algorithm is used in conjunction with the serial interference cancellation technique [13] to jointly *detect* and *estimate* the required multipath channel parameters such as the number of MPCs, their complex amplitudes, TOAs, and AOAs.[1] It was demonstrated that the FD-SAGE outperforms the standard SAGE algorithm [11] in a multipath rich environment in terms of its accuracy and stability [13]. The ML-based method is chosen in favor of the subspace-based method because of the advantages it offers as detailed in [14].

At each location, 1120 complex channel responses were recorded at each antenna element. By assuming that the channel is *quasistatic*,[2] averaging is carried out over the time-domain for each block of 16 snapshots. The resultant averaged complex channel responses are then operated on by the FD-SAGE algorithm to estimate the required parameters. Hence, 70 sets of channel parameters are obtained per location and can be assumed to be time-invariant (due to the quasistatic assumption) and are given by

$$\Theta_i = [\,\alpha_{l,i}\tau_{l,i}\phi_{l,i}\,], \quad l = 1,2,\ldots,L_i \text{ and } i = 1,2,\ldots,70 \quad (1)$$

where Θ_i is an $(L_i \times 3)$ matrix that contains the ith channel parameters set with L_i number of MPCs, while $\alpha_{l,i}$, $\tau_{l,i}$, and $\phi_{l,i}$ are the complex amplitude, TOA and AOA of the lth path in the ith parameter set, respectively. Subsequently, these were concatenated with respect to their corresponding domains, i.e., $\sum_{i=1}^{70}\sum_{l=1}^{L_i}\Theta_i$ to give a $(70L_i \times 3)$ resultant matrix. A cutoff threshold of 35-dB below the strongest path was applied to the concatenated data to ensure that only the effective MPCs are modeled since the useful dynamic range of the sounder is approximately 40 dB.

B. Cluster Identification

Measurement results from three scenarios reveal that the MPCs tend to form clusters in both the spatial and temporal domains. Therefore, the next task was to identify the clusters. Different researchers have different definitions of a cluster [15]–[17]. Here, we define a *cluster* as an accumulation of MPCs with similar TOAs and AOAs. The clustering phenomenon has been reported as a result of the superstructure (e.g., furniture, walls, doors, etc.) of the environment [5].

A nonparametric density estimation procedure, namely the kernel density estimate (KDE) technique [18], was deployed as an alternative to assist the clustering identification process. This

[1]AOA refers to the azimuthal angle only.

[2]The channel can be assumed to be invariant during this time interval.

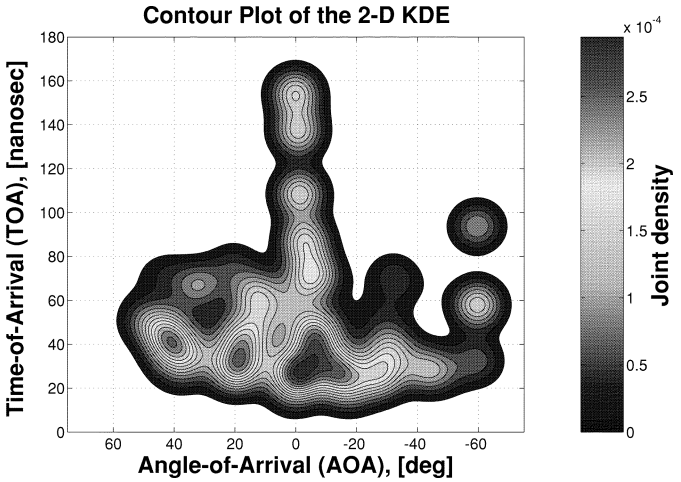

Fig. 3. MPC TOA-AOA contour plot after being processed by the 2-D KDE technique.

procedure is preferred due to its robustness, simplicity and convenience. Since clusters are observed in both the temporal and spatial domains, they need to be identified jointly in both domains. First, all MPCs within each data set are normalized with respect to the TOA of the first arrival path in order to remove the propagation effect due to the TX-RX separation and thus enabling various data sets to be compared. Then, the two-dimension (2-D) Gaussian KDE technique [18] was applied to each data set. Fig. 3 shows the MPC TOA-AOA contour plot of a sample data file after being processed by the 2-D KDE technique. This graph clearly shows that clustering exists in both the spatial and temporal domains. Clusters become more obvious after the KDE procedure and can be easily identified by visual inspection. Both [5] and [6] also deploy visual inspection to identify clusters from their measurement data.

IV. Spatio-Temporal Channel Model

In this section, we propose a new statistical wideband spatio-temporal channel model that incorporates both the clustering phenomenon and the spatio-temporal correlation properties. The model parameters are derived from the data collected during the measurement campaigns described in Section II and is particularly tailored for the HIPERLAN/2 and IEEE802.11a systems that employ SA architectures. By assuming a finite number of MPCs impinging on the antenna array, the clustering spatio-temporal channel model can be expressed as

$$h(\tau,\phi)=\sum_{k=1}^{K}\sum_{l=1}^{L_k}(R_k\cdot r_{kl})\cdot e^{j\varphi_{kl}} \cdot\delta\left(\tau-T_k-\tau_{kl},\phi-\Phi_k-\phi_{kl}\right) \quad (2)$$

where $\delta(\cdot)$ is the Dirac delta function, K is the number of clusters and L_k is the number of MPCs within the kth cluster. T_k, Φ_k, and R_k are the TOA, AOA, and amplitude of the kth cluster, which are defined as the TOA of the first arriving MPC, the mean AOA and the maximum amplitude of all MPCs within the kth cluster, respectively. While τ_{kl}, ϕ_{kl}, r_{kl}, and φ_{kl} are the TOA, AOA, amplitude and phase of the lth MPC in the kth cluster, respectively. The distribution of $\{\varphi_{kl}\}_{\substack{l\in L_k\\ k\in K}}$ is assumed to be statistically independent and uniform over the range of [0, 360]°. Notice that τ_{kl}, ϕ_{kl}, and r_{kl} are the relative values with respect to T_k, Φ_k, and R_k, respectively.

In reality, all of the parameters in (2) are randomly time-varying functions. However, the variations are very small compared with the signaling rate and it is, therefore, reasonable to assume them to be time-invariant random variables. The proposed channel model relies on two classes of parameters, namely, *intercluster* and *intracluster parameters* which characterize the cluster and the MPC, respectively. From (2), $\{K, T_k, \Phi_k, R_k\}$ and $\{L_k, \tau_{kl}, \phi_{kl}, r_{kl}, \varphi_{kl}\}$ are classified as the intercluster and intracluster parameters, respectively.

V. Statistical Characterization of the Channel Parameters

A. General Overview

This section presents the statistical characterization of the intercluster and intracluster channel parameters defined in Section IV. The variations of these parameters may be characterized statistically by fitting the measurement data against the proposed theoretical distributions. Three scenarios are considered covering LOS, OLOS, and NLOS conditions. Previous analysis showed that the statistical characteristics in OFF and LAB under LOS conditions are very similar [19]. Thus, unless otherwise stated, the LOS scenario corresponds to the OFF environment only.

B. Joint Distribution of Cluster Position

Clustering is observed in the temporal and angular domains. The 2-D joint pdf of cluster position, $f(T_k,\Phi_k)$ can be expressed as

$$f\left(T_k,\Phi_k\right)=f\left(\Phi_k|T_k\right)\cdot f\left(T_k\right) \quad (3)$$

where $f(\Phi_k|T_k)$ is the cluster conditional AOA pdf and $f(T_k)$ is the cluster marginal TOA pdf and Fig. 4 shows $f(T_k,\Phi_k)$ for the LOS and OLOS scenarios. $f(T_k,\Phi_k)$ of the NLOS scenario is not shown here due to its similarity in shape to the OLOS case. The angular axis for the LOS scenario spans from -60° to $+60^\circ$ while for the OLOS scenario, the angular axis spans from -180° to $+180^\circ$. The latter case is due to the concatenation of three rotations to form the 360° full spatial view. While under the LOS scenario, concatenation was not performed because the experimental results showed that majority of MPCs arrive within $\pm 60^\circ$ of the LOS direction. MPCs outside this angular range have much weaker power and are thus negligible.

These graphs reveal that there are significant differences between the joint spatio-temporal statistics of the LOS and the OLOS and NLOS scenarios. Under the LOS conditions, paths arriving at the RX with short delays can have a relatively large angular range, while paths which arrive with longer delays will have a much more restricted angle. This is because paths arriving at the RX with short delays are mainly due to the direct

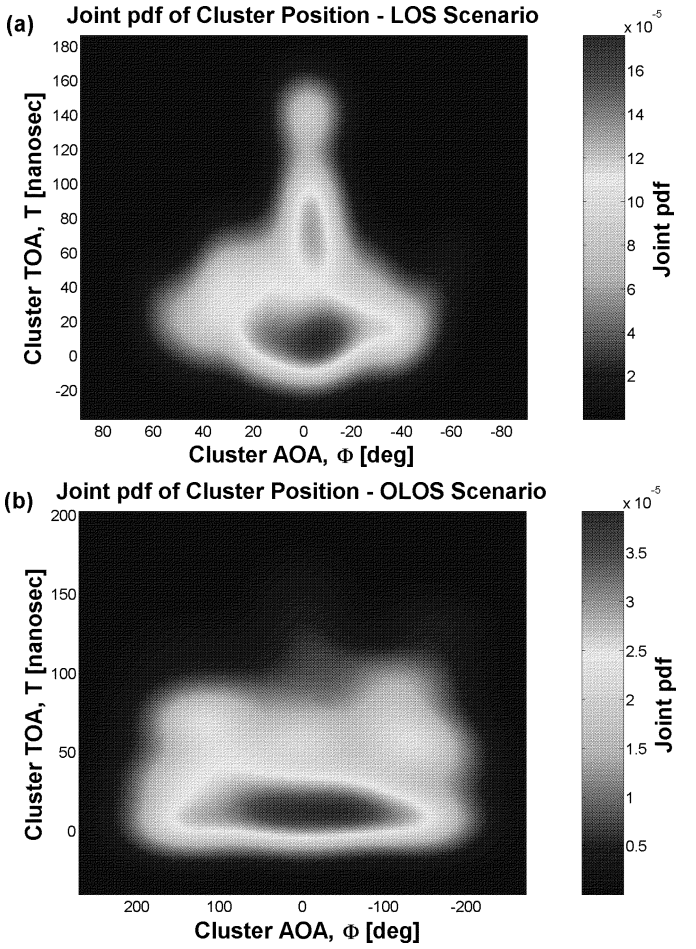

Fig. 4. Joint pdf of cluster position under (a) LOS and (b) OLOS scenarios.

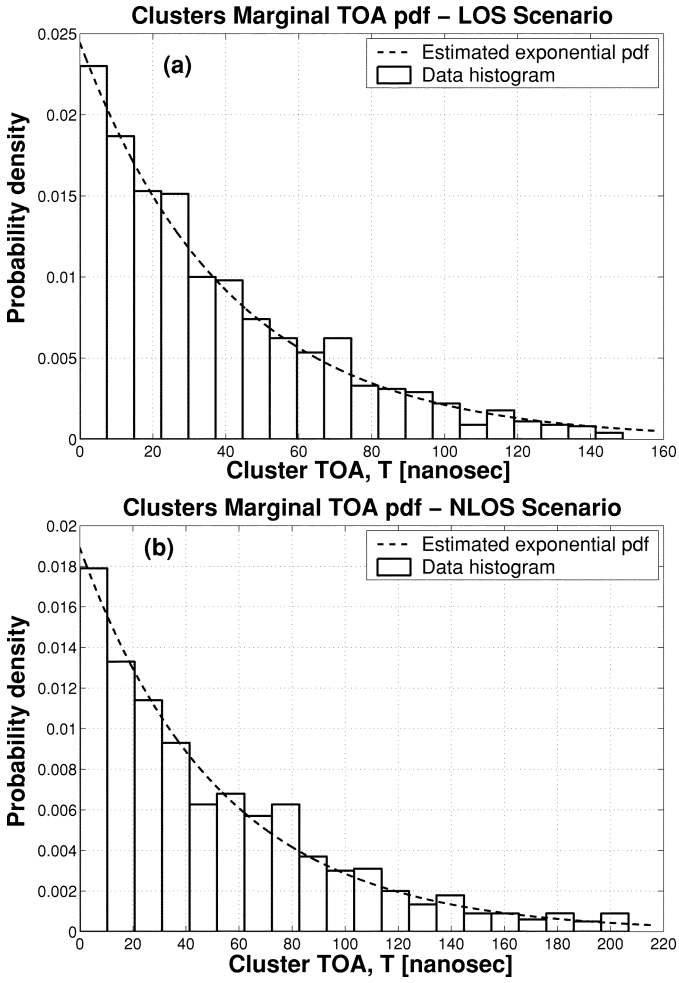

Fig. 5. Cluster marginal TOA pdf under (a) LOS and (b) NLOS scenarios.

path itself or reflections from the objects in the vicinity of the RX. These reflected paths can come from a large angular range as the RX may be surrounded by many reflecting objects. For example, paths reflected from the right and left walls in the office can have relatively large angular values, but with a small delay range. On the other hand, at larger delays, most paths arriving at the RX are effectively due to back-wall reflections (wall behind the TX). These paths have much lower powers, longer delays and angles very similar to the LOS direction. Generally, this is a result of the regular structure of the measurement environment [see Fig. 2(b)], which subsequently leads to the dependency between the spatial and temporal domains as show in Fig. 4(a).

Meanwhile under the OLOS scenario, the dependency between spatial and temporal domains becomes negligible. This is mainly due to the effect of obstructions to the direct path and some back-wall reflected paths caused by the wooden bookshelves and metal cabinets inside the office. The absence of these paths eliminates the clustered appearance at the short and long delay ranges in the LOS direction. Hence, reflected paths can come from any direction dependent on the location of the scatterers. Over a large number of locations, this phenomenon gives rise to the uniformly distributed cluster AOAs over the whole delay range as shown in Fig. 4(b). A similar argument is applicable to the NLOS scenario in which the direct path is completely blocked by the wall separating OFF and FOY. Due to this fact, it is reasonable to assume that the spatial and temporal domains are separable for the OLOS and NLOS scenarios by re-expressing (3) as follows:

$$f_{\mathrm{OLOS,NLOS}}\left(T_k, \Phi_k\right) = f\left(\Phi_k\right) \cdot f\left(T_k\right) \tag{4}$$

where $f(\Phi_k)$ is the cluster marginal AOA pdf which is approximately uniform over [0,360]°.

Arrival times have usually been modeled by the Poisson processes [5], [6]. The key feature of a Poisson process is the independence of events. However, due to the regular structure of the indoor environments, this assumption is rarely fulfilled in practice. Thus, in this paper, a more general approach is adopted. No *a priori* assumption on whether the arrival times satisfy a Poisson process or not is made. Instead, the arrival times are modeled by using a nonparametric estimation of the pdf based on the measurement data. The Anderson–Darling (A-D) goodness-of-fit test [20] was then used to verify the fitness of the chosen pdf. This approach also eases the extension of the proposed model to incorporate the dynamic evolution of the MPCs in the future. The cluster marginal TOA pdf, $f(T_k)$ was estimated by accumulating all clusters' AOAs, $\{\Phi_k\}_{k\in K}$. Fig. 5 shows the empirical cluster marginal TOA histogram density for

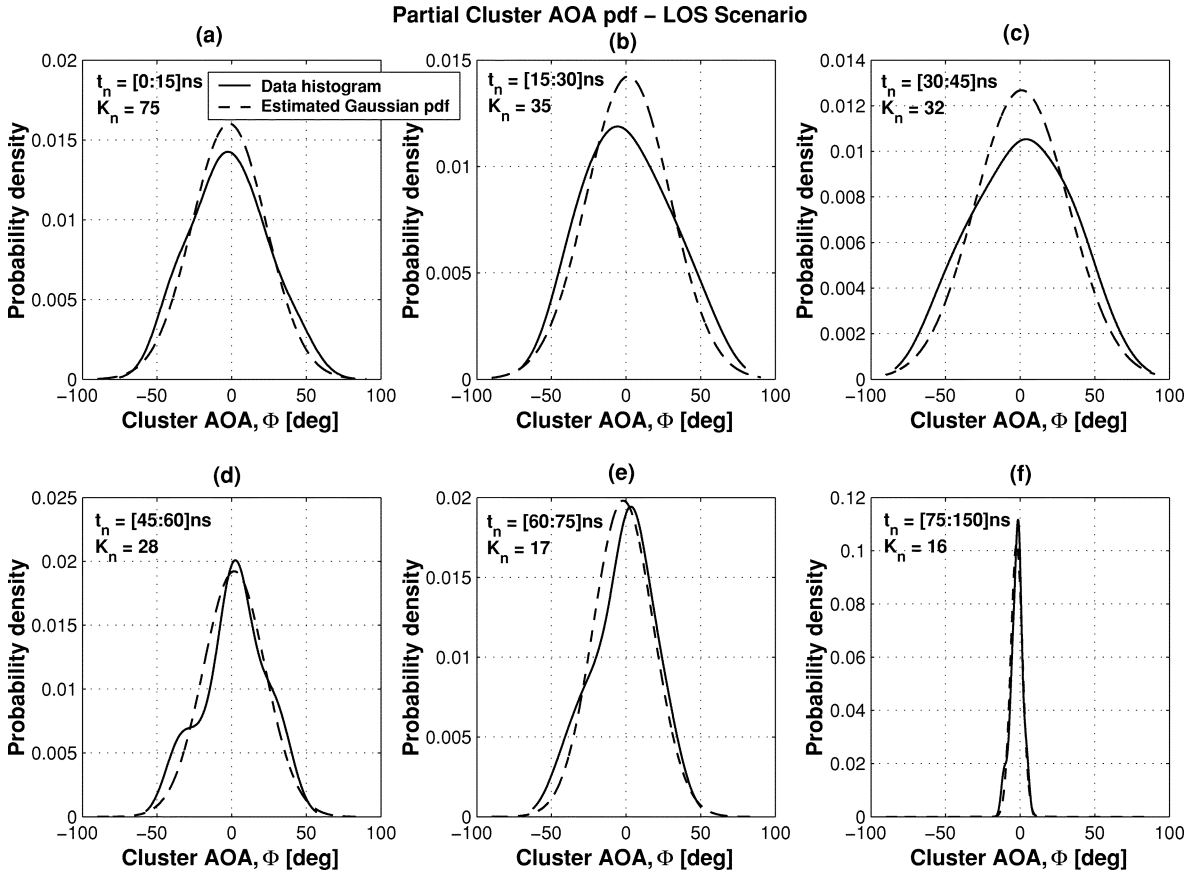

Fig. 6. Partial cluster conditional AOA pdf for each delay step under LOS scenario.

the LOS and NLOS scenarios with their estimated pdf plotted as solid curves. It is obvious that $f(T_k)$ can be well modeled by an exponential pdf given by

$$f(T_k) = \begin{cases} \frac{1}{\mu_T} \exp\left(-\frac{T_k}{\mu_T}\right), & T_k > 0 \\ 0, & \text{otherwise} \end{cases} \tag{5}$$

where μ_t is the mean value.

For the LOS scenario, it is necessary to estimate the cluster conditional AOA pdf, $f(\Phi_k|T_k)$. We adopt a new approach, in which the parameters of $f(\Phi_k|T_k)$ are described by an empirical formula that fits the measured data. We introduce the term partial cluster conditional AOA pdf $f(\Phi|t_n)$ which is associated with $f(\Phi_k|T_k)$ as follows:

$$f(\Phi_k|T_k) = \sum_{n=0}^{N-1} f(\Phi|t_n), \quad n \in \{0, 1, \ldots, N-1\} \tag{6}$$

where $t_n = n\Delta t \leq t_n < (n+1)\Delta t$, Δt is the delay step and N is the number of delay steps. Here, $\Delta t = 15$ ns was chosen in order to ensure that the number of clusters in each delay step, K_n was sufficient (i.e., at least 15) for further statistical analysis of $f(\Phi|t_n)$. By observing the shape of $f(\Phi|t_n)$ for $t_n \in \{t_0, t_1, \ldots, t_{N-1}\}$, a known pdf is proposed to represent the varying shape of $f(\Phi|t_n)$ by a change of its parameter values (normally the mean and standard deviation). It was noted that, at larger delay values, fewer clusters were observed. In order to obtain a good statistical representation, the number of samples has to be sufficiently large. This was achieved by increasing Δt at larger delays values. Fig. 6 shows a series of graphs of $f(\Phi|t_n)$ for $t_n \in \{t_0, t_1, \ldots, t_{N-1}\}$. The value of K_n to generate each of these graphs are also shown on the plot. In general, these graphs show that a Gaussian pdf can provide a reasonably good match. Therefore, a zero-mean[3] Gaussian pdf is proposed to model $f(\Phi|t_n)$ for $t_n \in \{t_0, t_1, \ldots, t_{N-1}\}$ which can be expressed as follows:

$$f(\Phi|t_n) = \frac{1}{\sqrt{2\pi} \cdot \sigma_{\Phi|t_n}} \exp\left\{-\frac{\Phi^2}{2\sigma^2_{\Phi|t_n}}\right\} \tag{7}$$

where $\sigma_{\Phi|t_n}$ is the standard deviation conditioned upon t_n. Its variation can be approximated by a Weibull distribution given by

$$\sigma_{\Phi|t_n}(t_n) = c_{\Phi|t_n} \cdot \left(\frac{t_n}{a_{\Phi|t_n}}\right)^{b_{\Phi|t_n}-1} \cdot \exp\left[-\left(\frac{t_n}{a_{\Phi|t_n}}\right)^{b_{\Phi|t_n}}\right] \tag{8}$$

where $a_{\Phi|t_n}$, $b_{\Phi|t_n}$, and $c_{\Phi|t_n}$ are the parameters for the Weibull distribution which were estimated using a nonlinear least squares regression method [21]. Notice that (8) is not the conventional Weibull pdf as the area under the curve does not necessarily equal one. Fig. 7 shows the empirical $\sigma_{\Phi|t_n}$ for $t_n \in \{t_0, t_1, \ldots, t_{N-1}\}$ and its least squares fit for the OFF and LAB.

[3]The mean value is zero because the LOS direction is taken as the reference, i.e., at 0°.

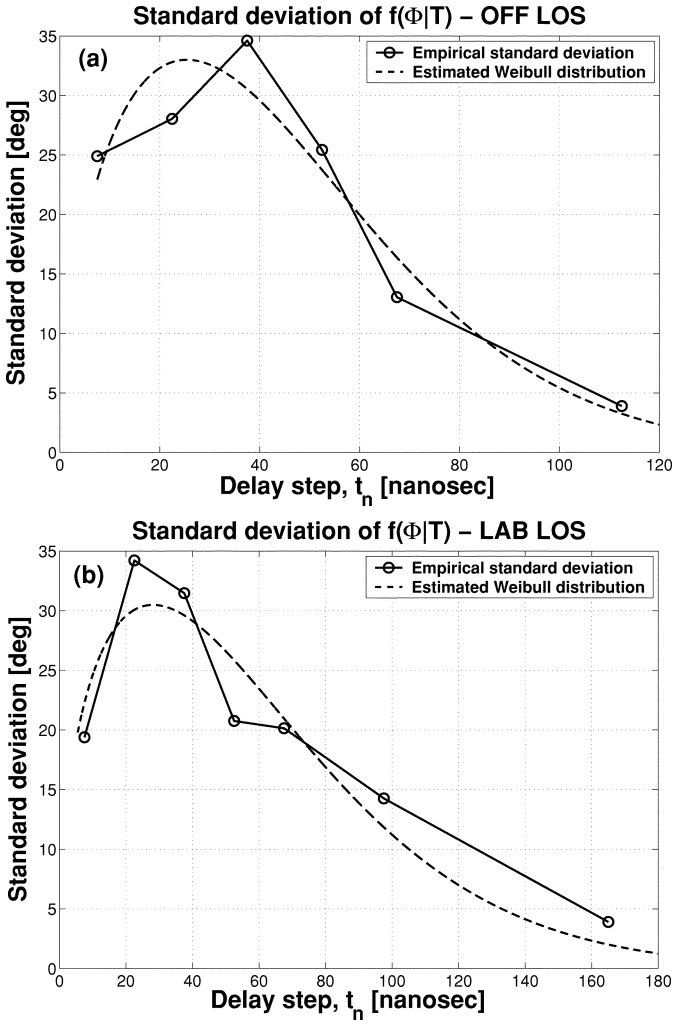

Fig. 7. Standard deviation of the cluster conditional AOA pdf as a function of delay step for (a) OFF-LOS and (b) LAB-LOS environments.

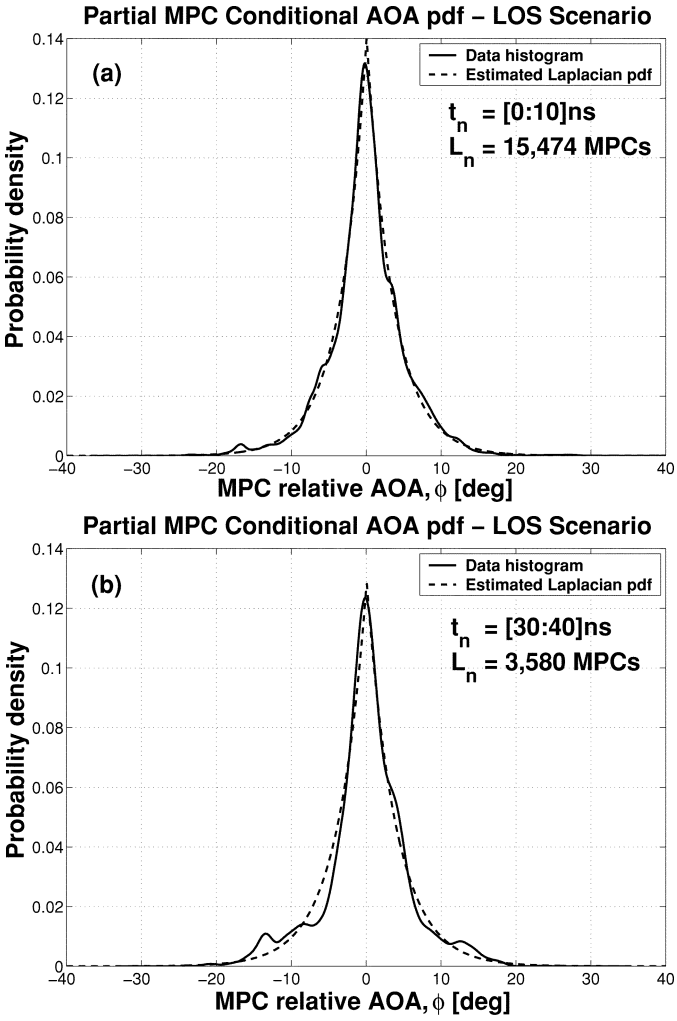

Fig. 8. Partial MPC conditional AOA pdf for two arbitrary chosen delay steps under LOS scenario.

C. Joint Distribution of MPCs Position Per Cluster

For the intracluster channel parameters, the 2-D joint pdf of MPCs position per cluster, $f(\tau_{kl}, \phi_{kl})$ can be expressed as

$$f(\tau_{kl}, \phi_{kl}) = f(\phi_{kl}|\tau_{kl}) \cdot f(\tau_{kl}) \tag{9}$$

where $f(\phi_{kl}|\tau_{kl})$ is the MPC conditional AOA pdf and $f(\tau_{kl})$ is the MPC marginal TOA pdf. Note that, $\{\tau_{kl}\}_{\substack{l\in L_k \\ k\in K}}$ and $\{\phi_{kl}\}_{\substack{l\in L_k \\ k\in K}}$ are the relative values with respect to their corresponding cluster position, i.e., $\{T_k\}_{k\in K}$ and $\{\Phi_k\}_{k\in K}$, respectively. Results from the data analysis show that $f(\tau_{kl})$ can be well modeled by an exponential pdf. This observation is in agreement with [7].

Using a similar approach as described in Section V-B, the partial MPC conditional AOA pdf, $f(\phi|t_n)$ is introduced and can be related to $f(\phi_{kl}|\tau_{kl})$ in a similar way as in (6) by replacing T_k, Φ_k and Φ with τ_{kl}, ϕ_{kl} and ϕ, respectively. Here, $\Delta t = 10$ ns is used instead to ensure that a sufficient number of MPCs is present in each delay step, L_n for statistical analysis of $f(\phi|t_n)$. Analysis results show that $f(\phi|t_n)$ for $t_n \in \{t_0, t_1, \ldots, t_{N-1}\}$ can be accurately modeled by a series of Laplacian pdfs with negligible variation in their standard deviations. Fig. 8 shows $f(\phi|t_n)$ for two arbitrary chosen delay steps, i.e., $t_n = [0 : 10]$ns and $t_n = [30 : 40]$ns, which further verify the observation results. The value of L_n to generate these two graphs is also given. Recall that a *cluster* is a group of MPCs with similar TOAs and AOAs. Hence, it is reasonable to assume that MPCs that belong to a particular cluster are due to reflections from the same object. Reflections from this object will create a fixed angular spread with respect to the RX position, irrespective of the absolute TOAs. Consequently, small changes in the path length will give rise to an insignificant variation in the angular domain. This explanation supports the results obtained for the constant standard deviation Laplacian pdfs described above. Thus, it is reasonable to assume that the intracluster spatial and temporal domains are independent of each other by re-expressing (9) as follows:

$$f(\tau_{kl}, \phi_{kl}) = f(\phi_{kl}) \cdot f(\tau_{kl}) \tag{10}$$

where $f(\phi_{kl})$ is the MPC marginal AOA pdf, given by the zero-mean Laplacian pdf

$$f(\phi_{kl}) = \frac{1}{\sqrt{2}\sigma_\phi} \exp\left\{-\sqrt{2}\frac{|\phi_{kl}|}{\sigma_\phi}\right\} \tag{11}$$

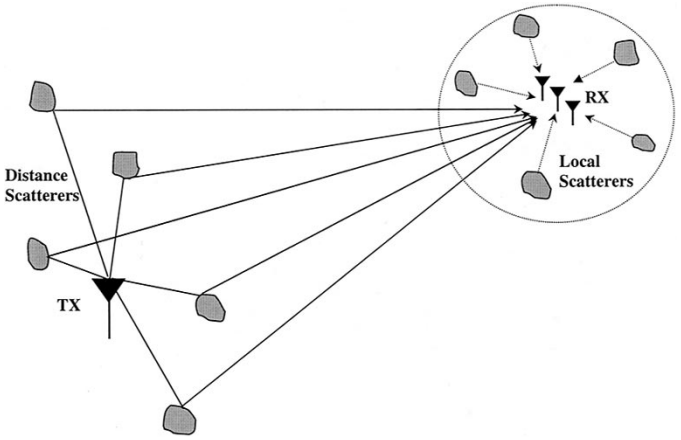

Fig. 9. Illustration of the effect of local and distance scatterers on the AOAs distribution at the RX.

with σ_ϕ is the standard deviation, which is the mean value of $\sigma_{\phi|t_n}$ for $t_n \in \{t_0, t_1, \ldots, t_{N-1}\}$. Notice that this simplification is also applicable for the OLOS and NLOS scenarios.

Several researchers [6], [7], [16] have reported that the Laplacian distribution can provide a good match to the distribution of the MPC AOAs. However, none of them explained why this distribution was chosen in favor of the others except that it fits the measurement data well. Here, the physical propagation mechanisms (*local* and *distance scatterers* effect) and the geometry of the measurement environments are related to show they can lead to a Laplacian shape of AOAs distribution at the RX. Fig. 9 illustrates the effect of the local and distance scatterers on the AOAs distribution at the RX. As depicted in the figure, the RX is surrounded by many local scatterers in its vicinity. Reflections due to the local scatterers can give rise to a large angular spread. On the other hand, distance scatterers are located much further away from the RX and reflected paths arriving at the RX are primarily from one particular direction through a much narrower angular spread. Assuming that there are same number of scatterers at both the TX and RX end and each of the scatterers give rise to the same number of paths. This phenomenon will cause a much higher density of paths at one particular direction and lower densities at other directions, which is similar to a Laplacian distribution with high occupancies at the center and lower occupancies at the larger angular values. Ertel and Reed [22] have derived AOA statistics based on uniformly distributed scatterers in the elliptical and circular regions. It showed that the AOA pdf for the elliptical scattering model approximates a Laplacian distribution. This observation further substantiates the above justification.

D. Number of Clusters and Distribution of the Number of MPCs Per Cluster

The average number of clusters per data set was approximately nine under the LOS and OLOS scenarios and seven for the NLOS scenario. Generally, these values are higher than those found by others, for example only 1–2 clusters in [5] and five clusters in [6]. The possible explanation is due to the use of the super-resolution FD-SAGE algorithm, which has high temporal and angular resolution capability in resolving closely spaced MPCs. On the other hand, the number of MPCs per cluster, L_k can be well modeled by an exponential pdf $f(L_k)$. In general, L_k increases from LOS to OLOS and NLOS scenarios and for 50% of the time, a cluster will contain less than five MPCs which implies that the channel is dominated by specular reflections.

The number of MPCs per cluster (thus, the number of clusters) is heavily dependent on the resolution of the parameter estimation algorithm (i.e., FD-SAGE algorithm in this case). To the best of the authors' knowledge, none of the existing algorithms is able to estimate all of the closely spaced MPCs within a cluster accurately. However, the resolution achieved by the FD-SAGE algorithm is far greater than the resolution limit imposed by the HIPERLAN/2 or IEEE802.11a systems. Hence, the model proposed here is generic and suitable for system simulation of both of these standards. Furthermore, the number of clusters and MPCs detected are also dependent on several other factors such as the TX-RX separation and location, the physical layout of the environment, as well as the dynamic range of the channel sounder. Fewer clusters and MPCs were observed at large TX-RX separations or when they were located in different rooms because at large TX-RX separations, MPCs impinging on the RX have a weaker power. If their path weights are beyond the useful dynamic range of the channel sounder, they will not be observable and thus reducing the number of effective clusters and MPCs. Meanwhile in a heavily cluttered environment, more clusters and MPCs were observed because many MPCs will undergo more complex propagation mechanisms such as multiple-order reflections, scattering, diffraction, etc.

VI. Channel Power Density Spectra

The channel PDS are used to characterize the channel impulse response. For a directional channel, this is characterized by the power-delay-azimuth density spectrum (PDADS), $P(\tau, \phi)$ given by

$$P(\tau, \phi) = E\left\{|h(\tau, \phi)|^2\right\} \tag{12}$$

where $E\{\cdot\}$ and $|\cdot|$ denote the expectation and absolute value, respectively. The clustering effect give rise to the intercluster PDADS, $P_{\text{Inter}}(T, \Phi)$ and the intracluster PDADS, $P_{\text{Intra}}(\tau, \phi)$, which describe the power density of clusters and MPCs, respectively, at a particular delay and angle.

Fig. 10 shows a series of superimposed curves for the empirical intercluster partial power-azimuth density spectrum (PADS), $P_{\text{Inter}}(\Phi|t_i)$ and the empirical intracluster partial PADS, $P_{\text{Intra}}(\phi|t_j)$ for $t_i \in \{25, 50, \ldots, 150\}$ns and $t_j \in \{10, 20, \ldots, 70\}$ns, respectively, under the LOS scenario. All partial PADS are normalized so that the maximum value is always one, which enables all curves to be superimposed for ease of comparison. These curves reveal that the variation of the standard deviation in both cases is negligible. Hence, $P_{\text{Inter}}(T, \Phi)$ and $P_{\text{Intra}}(\tau, \phi)$ can be simplified as two separable functions as follows

$$P_{\text{Inter}}(T, \Phi) = P_{\text{Inter}}(T) \cdot P_{\text{Inter}}(\Phi) \tag{13}$$

$$P_{\text{Intra}}(\tau, \phi) = P_{\text{Intra}}(\tau) \cdot P_{\text{Intra}}(\phi) \tag{14}$$

where $P_{\text{Inter}}(T)$ and $P_{\text{Intra}}(\tau)$ are the intercluster and intracluster power-delay density spectrum (PDDS), respectively,

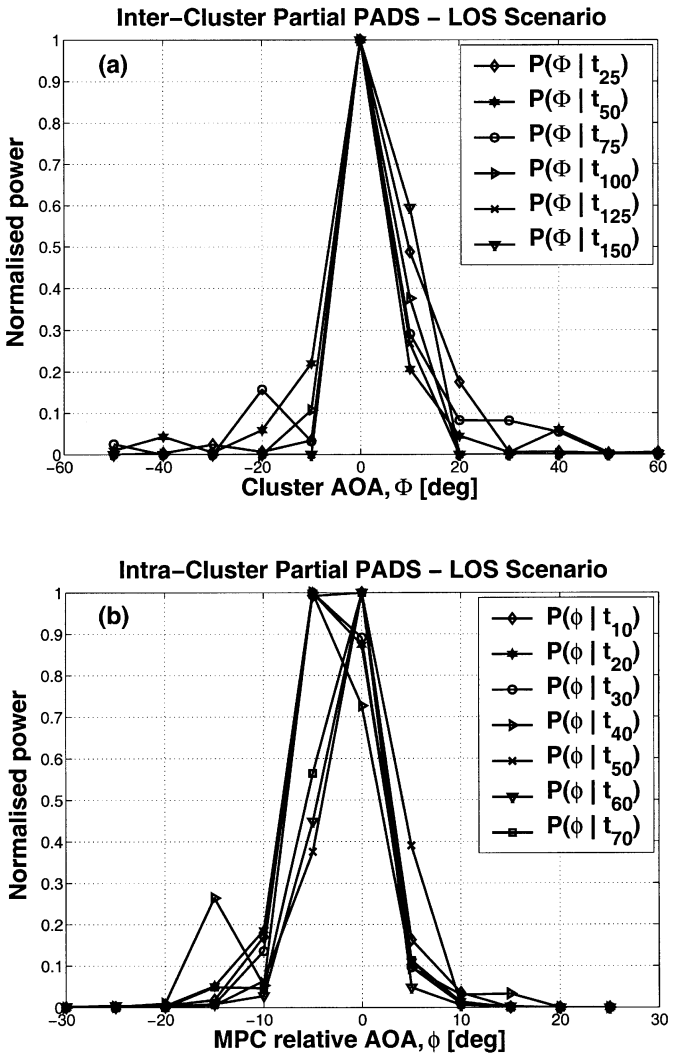

Fig. 10. (a) Empirical intercluster partial PADS and (b) empirical intracluster partial PADS, under the LOS scenario.

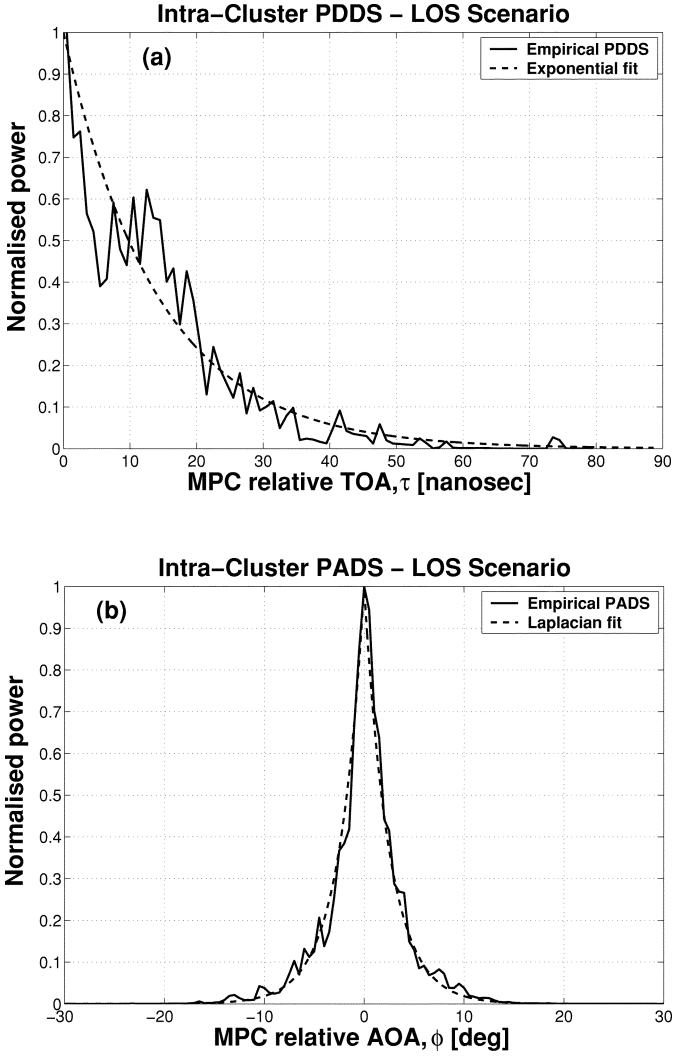

Fig. 11. (a) Intracluster PDDS and (b) intracluster PADS, under LOS scenario.

while $P_{\text{Inter}}(\Phi)$ and $P_{\text{Intra}}(\phi)$ are the intercluster and intracluster PADS, respectively. Due to the limited amount of data available here, this can only be an approximation. In order to gain further insight, a larger amount of data would be required.

Both $P_{\text{Inter}}(T)$ and $P_{\text{Intra}}(\tau)$ were estimated from the measurement data and were found to be accurately modeled by a decaying exponential function as follows

$$P_{\text{Inter}}(T) \propto \frac{1}{\tilde{\sigma}_T} \exp\left(-\frac{T}{\tilde{\sigma}_T}\right) \tag{15}$$

$$P_{\text{Intra}}(\tau) \propto \frac{1}{\tilde{\sigma}_\tau} \exp\left(-\frac{\tau}{\tilde{\sigma}_\tau}\right) \tag{16}$$

where $\tilde{\sigma}_T$ and $\tilde{\sigma}_\tau$ are the rms delay spread (DS) of $P_{\text{Inter}}(T)$ and $P_{\text{Intra}}(\tau)$, respectively. $P_{\text{Inter}}(T)$ was obtained by taking into account all the cluster powers, $\{R_k^2\}_{k\in K}$ and cluster TOAs, $\{T_k\}_{k\in K}$ while $P_{\text{Intra}}(\tau)$ was obtained by accumulating all MPCs relative powers, $\{r_{kl}^2\}_{\substack{l\in L_k \\ k\in K}}$ and MPCs relative TOAs, $\{\tau_{kl}\}_{\substack{l\in L_k \\ k\in K}}$. On the other hand, $P_{\text{Inter}}(\Phi)$ was found to be accurately modeled by a Laplacian function under the LOS scenario and uniformly distributed over the range of [0, 360]° for the OLOS and NLOS scenarios. Meanwhile, $P_{\text{Intra}}(\phi)$ was found to be well modeled by a Laplacian function for all three scenarios. The Laplacian function for $P_{\text{Inter}}(\Phi)$ (LOS scenario only) and $P_{\text{Intra}}(\phi)$ are given as follows

$$P_{\text{Inter}}(\Phi) \propto \frac{1}{\sqrt{2}\tilde{\sigma}_\Phi} \exp\left(-\sqrt{2}\frac{|\Phi|}{\tilde{\sigma}_\Phi}\right) \tag{17}$$

$$P_{\text{Intra}}(\phi) \propto \frac{1}{\sqrt{2}\tilde{\sigma}_\phi} \exp\left(-\sqrt{2}\frac{|\phi|}{\tilde{\sigma}_\phi}\right) \tag{18}$$

where $\tilde{\sigma}_\Phi$ and $\tilde{\sigma}_\phi$ is the rms azimuth spread (AS) of $P_{\text{Inter}}(\Phi)$ and $P_{\text{Intra}}(\phi)$, respectively. Likewise, $P_{\text{Inter}}(\Phi)$ and $P_{\text{Intra}}(\phi)$ is the accumulation of $\{R_k^2\}_{k\in K}$ at $\{\Phi_k\}_{k\in K}$ and $\{r_{kl}^2\}_{\substack{l\in L_k \\ k\in K}}$ at $\{\phi_{kl}\}_{\substack{l\in L_k \\ k\in K}}$, respectively. Fig. 11 shows $P_{\text{Intra}}(\tau)$ and $P_{\text{Intra}}(\phi)$ for the LOS scenario. The estimated exponential and Laplacian functions (dashed curves) were also plotted on the empirical power spectra (solid curves) and their parameters were estimated using the least squares method. Exponential PDDS and Laplacian PADS are also reported in [23] for the macrocell outdoor environment.

TABLE I
CHANNEL PARAMETERS OF THE INTERCLUSTER AND INTRACLUSTER PDFS AND POWER DENSITY SPECTRA AND COMPARISON WITH THE ESVM AND SRCM MODEL PARAMETERS

Parameter	LOS	OLOS	NLOS	ESVM	SRCM
Mean of $f(\mathrm{T}_k)$, μ_T	40.88 ns	41.15 ns	52.87 ns	-	14.70 ns
$a_{\Phi l_n}$ } Parameters for the Weibull distribution	50.16	-	-	-	-
$b_{\Phi l_n}$ } Parameters for the Weibull distribution	1.54	-	-	-	-
$c_{\Phi l_n}$ } Parameters for the Weibull distribution	67.71	-	-	-	-
Mean of $f(L_k)$, μ_L	1.64	4.09	5.22	-	-
Mean of $f(\tau_{kl})$, μ_τ	13.76 ns	22.00 ns	33.35 ns	-	15.80 ns
Standard deviation of $f(\phi_{kl})$, σ_ϕ	3.93°	9.03°	7.32°	26.00°	19.50°
RMS DS of $P_{Inter}(\mathrm{T})$, $\tilde{\sigma}_\mathrm{T}$	6.52 ns	9.21 ns	10.88 ns	34.00 ns	11.20 ns
RMS DS of $P_{Intra}(\tau)$, $\tilde{\sigma}_\tau$	13.37 ns	19.09 ns	37.93 ns	29.00 ns	11.60 ns
RMS AS of $P_{Inter}(\Phi)$, $\tilde{\sigma}_\Phi$	6.83°	-	-	-	-
RMS AS of $P_{Intra}(\phi)$, $\tilde{\sigma}_\phi$	3.31°	9.02°	9.49°	-	18.50°

VII. COMPARISON WITH OTHER MODELS

Channel parameters of all of the proposed pdfs and PDS extracted from the measurement data for all three scenarios are given in Table I. Also listed in the table are the channel parameters for the ESVM and SRCM models introduced earlier. Notice that both models were derived from the measurement data collected under the NLOS scenario. Parameters given for the ESVM model correspond to the Clyde Building [6]. In general, the temporal parameters of the new proposed model (NLOS scenario only) are larger than the values obtained by both ESVM and SRCM except for $\tilde{\sigma}_T$, which is approximately the same as the value from SRCM but less than the value from ESVM. The possible explanation for these discrepancies is due to several factors such as the physical structure and size of the room, the TX-RX separation, as well as buildings construction. On the other hand, the angular parameters obtained are much smaller than the values given by both ESVM and SRCM. The azimuth dispersion is dependent on the resolution capability of the AOA estimation technique and the degree of clutter of the environment under consideration. The use of a super-resolution technique to estimate MPC AOAs in the SRCM and the model proposed here is one reason for the smaller angular spread obtained as compared with the ESVM model. Meanwhile, the higher degree of clutter in the environment where the SRCM was derived is the likely explanation for the larger azimuth dispersion obtained.

VIII. CONCLUSION

A new statistical wideband spatio-temporal indoor channel model has been proposed based on the measurement data collected at the 5.2-GHz band in three different scenarios—LOS, OLOS, and NLOS. The proposed model incorporates the spatio-temporal clustering phenomenon observed in the measurement data, as well as the correlation between these two domains. The super-resolution FD-SAGE algorithm is deployed to extract the MPC parameters prior to cluster identification using a nonparametric density estimation procedure.

A detailed statistical characterization of the model parameters was described, which include the average number of clusters, the MPCs distribution within a cluster and the joint pdf for the cluster and MPC positions. The main contribution of the paper is the introduction of these joint pdfs which fully describe the intercluster and intracluster spatio-temporal correlation properties. Such investigation has not been considered in detail as most previous researchers have assumed these two domains to be independent *a priori*. The modeling approach described here combines the pdfs of the channel parameters, which define the stochastic properties of the channel, with its channel PDS. The channel spatial and temporal PDS are also derived from measurement data and have been found to be well modeled by exponential and Laplacian functions, respectively. By having both the statistical pdfs and PDS, the channel can be easily reproduced by computer simulation. The validity of the new model is evaluated by comparing its parameters with two other models reported in the literature. Analysis results show that the *a priori* assumption concerning the independence between the spatial and temporal domains made by the ESVM and SRCM is appropriate only under the OLOS and NLOS scenarios. However, under the LOS scenario these two models fail to model the channel well due to the dependency that exists between the spatio-temporal domains.

Since the channel model developed in this work is focused on the indoor (picocell) WLAN application based around 5 GHz, the measurement for supporting the statistical analysis of the channel was conducted in the 5-GHz band. Hence, the proposed model is most suitable for simulating any HIPERLAN/2 and IEEE802.11a systems that employ smart antenna architectures, as well as for the evaluation of space–time processing applications in the indoor environment. However, we expect the statistical property of the channel to be different for other frequency bands (e.g., 2.4, 40, and 60 GHz) since the pathloss, AOA analysis, and radiowave propagation mechanisms are dependent on the carrier wavelength.

ACKNOWLEDGMENT

The authors would like to acknowledge Dr. D. Kitchener (Nortel Networks U.K. Ltd.) and Dr. D. Raynes (Philips Research Laboratory, U.K.) for their useful comments and suggestions.

REFERENCES

[1] A. Doufexi, S. Armour, M. Butler, A. Nix, D. Bull, J. McGeehan, and P. Karlsson, "A comparison of the HIPERLAN/2 and IEEE802.11a wireless LAN standards," *IEEE Commun. Mag.*, vol. 40, pp. 172–180, May 2002.

[2] A. F. Naguib, A. Paulraj, and T. Kailath, "Capacity improvement with base-station antenna arrays in cellular CDMA," *IEEE Trans. Veh. Technol.*, vol. 43, pp. 691–698, Aug. 1994.

[3] R. B. Ertel, P. Cardieri, K. W. Sowerby, T. S. Rappaport, and J. H. Reed, "Overview of spatial channel models for antenna array communication systems," *IEEE Pers. Commun.*, vol. 5, pp. 10–22, Feb. 1998.

[4] U. Martin, J. Fuhl, I. Gaspard, M. Haardt, A. Kuchar, C. Math, A. F. Molisch, and R. Thomä, "Model scenarios for direction-selective adaptive antennas in cellular mobile communication systems—Scanning the literature," *Kluwer Wireless Personal Communications*, vol. 11, no. 1, pp. 109–129, Oct. 1999.

[5] A. A. M. Saleh and R. A. Valenzuela, "A statistical model for indoor multipath propagation," *IEEE J. Select. Areas Commun.*, vol. 5, pp. 128–137, Feb. 1987.

[6] Q. H. Spencer, B. D. Jeffs, M. A. Jensen, and A. L. Swindlehurst, "Modeling the statistical time and angle of arrival characteristics of an indoor multipath channel," *IEEE J. Select. Areas Commun.*, vol. 18, pp. 347–359, Mar. 2000.

[7] R. Heddergott, "Stochastic Model for Mobile Radio Channels in Indoor Environments," Ph.D. (in German), Swiss Federal Institute of Technology Zurich, Zurich, Switzerland, 2000.

[8] J. Medbo, H. Andersson, P. Schramm, H. Asplund, and J.-E. Berg, "Channel Models for HIPERLAN/2 in Different Indoor Scenarios,", Bradford, U.K., Tech. Rep. COST 259 TD(98)070, 1998.

[9] K.-H. Li, M. A. Ingram, and A. V. Nguyen, "Impact of clustering in statistical indoor propagation models on link capacity," *IEEE Trans. Commun.*, vol. 50, pp. 521–523, Apr. 2002.

[10] R. S. Thomä, D. Hampicke, A. Richter, G. Sommerkorn, A. Schneider, U. Trautwein, and W. Wirnitzer, "Identification of time-variant directional mobile radio channels," *IEEE Trans. Instrum. Meas.*, vol. 49, pp. 357–364, Apr. 2000.

[11] B. H. Fleury, M. Tschudin, R. Heddergott, D. Dahlhaus, and K. I. Pedersen, "Channel parameter estimation in mobile radio environments using the SAGE algorithm," *IEEE J. Select. Areas Commun.*, vol. 17, pp. 438–450, Mar. 1999.

[12] M. Haardt and J. A. Nossek, "Unitary ESPRIT: How to obtain increased estimation accuracy with a reduced computational burden," *IEEE Trans. Signal Processing*, vol. 43, pp. 1232–1242, May 1995.

[13] C. C. Chong, D. I. Laurenson, C. M. Tan, S. McLaughlin, M. A. Beach, and A. R. Nix, "Joint detection-estimation of directional channel parameters using the 2-D frequency domain SAGE algorithm with serial interference cancellation," in *Proc. IEEE Int. Conf. Communications (ICC 2002)*, vol. 2, New York, USA, Apr. 2002, pp. 906–910.

[14] H. Krim and M. Viberg, "Two decades of array signal processing research," *IEEE Signal Processing Mag.*, vol. 13, pp. 67–94, July 1996.

[15] M. Toeltsch, J. Laurila, K. Kalliola, A. F. Molisch, P. Vainikainen, and E. Bonek, "Statistical characterization of urban spatial radio channels," *IEEE J. Select. Areas Commun.*, vol. 20, pp. 539–549, Apr. 2002.

[16] J. E. Dietert and B. Rembold, "Stochastic channel model for outdoor applications based on raytrace simulations," in *Proc. of the Millennium Conf. on Antennas and Propagation (AP2000)*, Davos, Switzerland, Apr. 2000.

[17] M. Steinbauer, "The Radio Propagation Channel—A Non-Directional, Directional and Double-Directional Point-of-View," Ph.D. dissertation, Tech. Univ. Vienna, Vienna, Austria, 2001.

[18] D. W. Scott, *Multivariate Density Estimation: Theory, Practice and Visualization*. New York: Wiley, 1992.

[19] C. C. Chong, D. I. Laurenson, and S. McLaughlin, "Statistical characterization of the 5.2 GHz wideband directional indoor propagation channels with clustering and correlation properties," in *Proc. IEEE Vehicular Technology Conf. (VTC 2002-Fall)*, vol. 1, Vancouver, BC, Canada, September 2002, pp. 629–633.

[20] R. B. D'Agostino and M. A. Stephens, *Goodness-of-Fit Techniques*. New York: Marcel Dekker, Inc., 1986.

[21] G. A. F. Seber, *Nonlinear Regression*. New York: Wiley, 1989.

[22] R. B. Ertel and J. H. Reed, "Angle and time of arrival statistics for circular and elliptical scattering models," *IEEE J. Select. Areas Commun.*, vol. 17, pp. 1829–1840, Nov. 1999.

[23] K. I. Pedersen, P. E. Mogensen, and B. H. Fleury, "A stochastic model of the temporal and azimuthal dispersion seen at the base station in outdoor propagation environments," *IEEE Trans. Veh. Technol.*, vol. 49, pp. 437–447, Mar. 2000.

Chia-Chin Chong (S'00) was born in Kuala Lumpur, Malaysia, on March 9, 1978. She received the B.Eng. degree with first class honors in electrical and electronics engineering from the University of Manchester, Manchester, U.K., in July 2000. Since August 2000, she has been with Institute for Digital Communications, the University of Edinburgh, Edinburgh, U.K., working toward the Ph.D. degree.

She also participated in the European COST 273 action, Toward Mobile Broadband Multimedia Networks. Her current research interests include wireless propagation channel measurements, characterization and modeling for indoor environments, and multidimensional channel parameters estimation.

Miss Chong received the Joseph Higham Prize and the GEC-Marconi Prize from the University of Manchester in 2000 for academic excellence and outstanding performance. She also was awarded the IEE Prize and the IEE Vodafone Scholarship by the Institution of Electrical Engineers (IEE), in 1999 and 2001, respectively, and the Richard Brown Scholarship from the University of Edinburgh in 2002. She is a Member of the IEE.

Chor-Min Tan (S'99) received the M.Sc. degree in electrical and electronic engineering from the University of Bristol, Bristol, U.K., in 2000, and is currently with the Centre for Communications Research working toward the Ph.D. degree.

He is also a Member in the European COST 273 Action. His research interests lie in the areas of multidimensional array signal processing techniques, indoor and outdoor high-resolution propagation measurement campaigns, and MIMO channel characterization and modeling.

Mr. Tan was awarded the DTI Radio Communication Agency Award and the first prize in the IEE Short Papers Presentation in 2000. He is a Member of the IEE and the IEICE.

David I. Laurenson (M'90) received the B.Eng. degree in computer science and electronics and the Ph.D. degree in electrical engineering, both from the University of Edinburgh, Edinburgh, U.K., in 1990 and 1994, respectively.

He has been a Lecturer in the University of Edinburgh since 1995 and is currently active in the fields of mobile communication channel modeling, resource metric estimation, and wireless ad hoc networks.

Stephen McLaughlin (M'84) was born in Clydebank, Scotland, U.K., in 1960. He received the B.Sc. degree in electronics and electrical engineering from the University of Glasgow, Glasgow, U.K., in 1981, and the Ph.D. degree from the University of Edinburgh, Edinburgh, U.K., in 1989.

From 1981 to 1984, he was a Development Engineer with Barr and Stroud Ltd., Glasgow, involved in the design and simulation of integrated thermal imaging and fire control systems. From 1984 to 1986, he worked on the design and development of high-frequency data communication systems with MEL Ltd. In 1986, he joined the Department of Electronics and Electrical Engineering, University of Edinburgh as a Research Fellow where he studied the performance of linear adaptive algorithms in high noise and nonstationary environments. In 1988, he joined the academic staff at the University of Edinburgh and from 1991 until 2001, he held a Royal Society University Research Fellowship to study nonlinear signal processing techniques.

Prof. McLaughlin was awarded a personal Chair in Electronic Communication Systems at the University of Edinburgh, in 2002. His research interests lie in the fields of adaptive signal processing and nonlinear dynamical systems theory and their applications to biomedical and communication systems.

Mark A. Beach (A'89) received the Ph.D. degree from the University of Bristol, Bristol, U.K., in 1989.

He then joined the Department of Electrical and Electronic Engineering, University of Bristol as a Member of academic staff. His research interests include smart antenna technology for wireless, as well as analogue RF circuitry for software definable radio (SDR). Examples include contributions to the European collaborative projects, TSUNAMI, SATURN, ROMANTIK, TRUST, and more recently SCOUT. At present his interests are focused toward multiple-input–multiple-output (MIMO) channel characterization and the design and optimization of space–time coded wireless architectures for 3G and 4G wireless networks.

Dr. Beach holds the post of Reader in Communication Systems at the University of Bristol. He is a Member of the IEE and an active Member of the IEE Professional Network on Antennas and Propagation, as well as an Editor for the IEEE TRANSACTIONS ON WIRELESS COMMUNICATIONS.

Andrew R. Nix (A'97) received the B.Eng. and Ph.D. degrees from the University of Bristol, Bristol, U.K., in 1989 and 1993, respectively.

He is currently Professor of Wireless Communication Systems at the University of Bristol. His main research interests include broadband wireless communications, radiowave propagation modeling, cellular network optimization, and advanced digital modulation/reception techniques. He currently leads the propagation modeling and wireless local-area network (WLAN) groups in the Centre for Communications Research (CCR). He has published in excess of 190 journals and conference papers.